

XIV. DETECTION AND ESTIMATION THEORY

Academic Research Staff

Prof. Arthur B. Baggeroer

Graduate Students

Steven J. Leverette
Louis S. Metzger

John W. Moffett
José M. F. Moura
Steen A. Parl

Leroy C. Pusey
Kenneth B. Theriault

A. ROLE OF THE STATIONARITY EQUATION OF LEAST-SQUARES LINEAR FILTERING IN SPECTRAL ESTIMATION AND WAVE PROPAGATION

Joint Services Electronics Program (Contract DAAB07-71-C-0300)
National Science Foundation (Grant GX-36331)

Leroy C. Pusey, Arthur B. Baggeroer

1. Introduction

It is well known that the least-squares linear estimate of a signal in additive white noise may be obtained by solving a Wiener-Hopf integral equation for the least-squares filter.¹ This report presents some new results concerning this integral equation and demonstrates that the observed process is wide-sense stationary if and only if the filter satisfies a certain differential equation referred to as the stationarity equation.

We indicate how these results may be applied to spectral estimation and to wave propagation in a lossless nonhomogeneous medium. We also interpret the Chandrasekhar equations^{2,3} in terms of the stationarity equation. Some of our results are analogous to certain well-known results in the linear predictive filtering of discrete-time processes.

2. Stationarity Equation

We summarize our results concerning the Wiener-Hopf type of integral equation,

$$h(t, \tau) + \int_0^t h(t, x) \beta(x, \tau) dx = \beta(t, \tau), \quad 0 \leq \tau \leq t \leq T. \quad (1)$$

We form the definitions:

1. An innovations kernel on $[0, T]$ is a continuous symmetric function $\beta(\mu, \nu)$, $0 \leq \mu, \nu \leq T$ such that $\delta(\mu-\nu) + \beta(\mu, \nu)$ is positive definite.

2. An innovations kernel is said to be stationary if it depends only on the difference of its two arguments. In this case, we write it as $\beta(\tau)$, $|\tau| \leq T$.

JS

JS

(XIV. DETECTION AND ESTIMATION THEORY)

JS

3. A Volterra kernel on $[0, T]$ is a function $h(t, \tau)$, $0 \leq \tau, t \leq T$ that is continuous on the triangle $0 \leq \tau \leq t \leq T$ and zero outside the triangle.

We employ the following result of Kailath:⁴

Eq. 1 determines a one-one correspondence between the innovations kernels on $[0, T]$ and the Volterra kernels on $[0, T]$.

We note that the mapping $\beta(\mu, \nu) \rightarrow h(t, \tau)$ is well known in the context of least-squares linear filtering theory (especially when $\beta(\mu, \nu)$ is a covariance function). Kailath has shown the following identity:

$$\beta(\mu, \nu) = b(\mu, \nu) + \int_0^\nu b(\mu, x) b(\nu, x) dx, \quad \mu \geq \nu, \tag{2}$$

where $b(\mu, \nu)$ is the sum of the Neumann series

$$\begin{aligned} b(\mu, \nu) = & h(\mu, \nu) + \int_\nu^\mu h(\mu, x_1) h(x_1, \nu) dx_1 \\ & + \int_\nu^\mu \int_\nu^{x_2} h(\mu, x_2) h(x_2, x_1) h(x_1, \nu) dx_1 dx_2 \\ & + \dots \quad 0 \leq \mu \leq \nu \leq T. \end{aligned} \tag{3}$$

Now, if $h(t, \tau)$ is a given Volterra kernel, it is easy to verify that the function $\beta(\mu, \nu)$ defined by (2) and (3) is an innovations kernel that satisfies (1). Thus, the inverse mapping $h(t, \tau) \rightarrow \beta(\mu, \nu)$ is well defined and Kailath's result follows.

We can show that

R1. An innovations kernel is stationary if and only if the corresponding Volterra kernel satisfies the differential equation

$$\frac{\partial}{\partial t} h(t, t-\tau) = -h(t, \tau) h(t, 0), \quad 0 \leq \tau \leq t \leq T. \tag{4}$$

For obvious reasons, we refer to (4) as the stationarity equation. This equation is the continuous-time analog of the Levinson recursion which is commonly employed in linear predictive filtering of discrete-time stationary processes.^{5, 6}

We have the following results pertaining to (4):

R2. For any continuous function $g(t)$, $0 \leq t \leq T$, the boundary-value problem composed of (4) and the boundary condition $h(t, 0) = g(t)$, $0 \leq t \leq T$ has a unique solution $h(t, \tau)$, where the latter is a Volterra kernel given by the uniformly convergent series

$$h(t, \tau) = \sum_{n=0}^{\infty} (-1)^n f_n(\tau, t-\tau), \quad 0 \leq \tau \leq t \leq T, \tag{5}$$

JS

where $f_0(x, \tau) = g(\tau)$, and

$$f_n(x, \tau) = \int_0^x f_{n-1}(\tau, y) g(y+\tau) dy, \quad n \geq 1.$$

R3. If $h(t, \tau)$ is a Volterra kernel satisfying (4), then the Laplace transform

$$R(s; \mu) = 1 - \int_0^\mu h(\mu, \mu-x) e^{-sx} dx \quad (s = \sigma + j\omega) \quad (6)$$

is bounded away from zero in the right-half s plane:

$$|R(s; \mu)| \geq \exp\left(-\int_0^\mu |g(t)| dt\right), \quad \sigma \geq 0, \quad 0 \leq \mu \leq T, \quad (7)$$

where $g(t) = h(t, 0)$, $0 \leq t \leq T$.

R2 and R3 are analogous to well-known results in discrete-time linear predictive filtering. The analogy to R2 is that, given the partial correlation coefficients, one may solve the Levinson recursion for the regression filter (one-step predictive error filter) and the analogy to R3 is that the regression filter is minimum-phase.⁵

We observe that R1-R2 imply that (1) determines a one-one correspondence between the stationary innovations kernels on $[0, T]$ and the continuous functions on $[0, T]$. We denote this correspondence by the invertible map

$$f_T: \beta(\tau), \quad |\tau| \leq T \rightarrow h(t, 0), \quad 0 \leq t \leq T.$$

It follows from (1) that f_T is "memoryless" in that an extension of $\beta(\tau)$ from the interval $[-T, T]$ to $[-T', T']$ yields a corresponding extension of $h(t, 0)$. Thus we have the following result:

R4. If $\beta(\tau)$, $|\tau| \leq T$ is an innovations kernel and $h(t, \tau)$ is the corresponding Volterra kernel, then the positive-definite continuous extensions $k^E(\tau)$, $|\tau| < \infty$ of the covariance $k(\tau) = \delta(\tau) + \beta(\tau)$ are equivalent to the continuous extensions of $h(t, 0)$, $0 \leq t \leq T$.

We have illustrated this result in Fig. XIV-1.

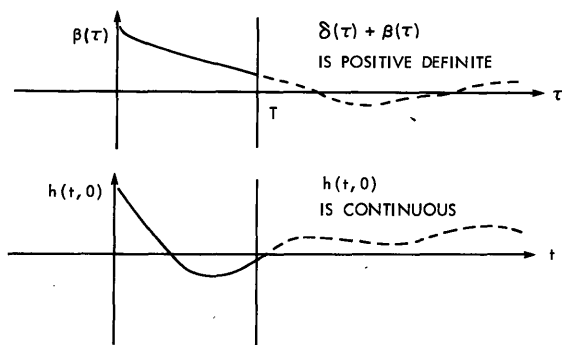


Fig. XIV-1.
Positive-definite extensions.

We now consider several applications of these results. We shall see that R2 and R3 may be applied to solve a certain distributed-state variable equation that arises when we consider wave propagation and which is directly related to the Chandrasekhar equations. First, we discuss the application of R4 to spectral estimation.

3. A Generalization of the Maximum Entropy Method

Suppose that we have covariance measurements of the form

$$k(\tau) = N_0 [\delta(\tau) + \beta(\tau)], \quad |\tau| \leq T,$$

where $N_0 > 0$ and $\beta(\tau)$ is an innovations kernel. If E represents the class of positive-definite continuous extensions of $k(\tau)$, then a logical way to estimate the power density spectrum is to select an element of E subject to some criterion. Because of the difficult constraint of positive definiteness, this approach has not been considered in the past. By R4, however, the problem reduces to choosing a continuous extension of $h(t, 0)$, $0 \leq t \leq T$.

This approach is a generalization of the maximum entropy method (M. E. M.) of spectral estimation,⁷⁻¹⁰ whereby the estimated covariance is extended by fitting an autoregressive process to the measurements. We can argue that the M. E. M. is equivalent to the zero extension of $h(t, 0)$, $0 \leq t \leq T$.

4. Solution to a Distributed-State Equation

Consider the complex distributed-state equation ($s = \sigma + j\omega$):

$$\frac{\partial}{\partial \mu} \underline{x}(\mu, s) = \underline{A}(\mu, s) \underline{x}(\mu, s), \quad 0 \leq \mu \leq T, \quad (8)$$

where

$$\underline{A}(\mu, s) = \begin{bmatrix} 0 & -g(\mu) e^{-s\mu} \\ -g(\mu) e^{s\mu} & 0 \end{bmatrix}$$

and $g(\mu)$, $0 \leq \mu \leq T$ is real-valued and continuous. We shall relate this equation to wave propagation on a nonuniform lossless transmission line and then compare (8) with the Chandrasekhar equations. It is of interest here that the solution to (8) follows from R2 and R3:

Let $R(s;\mu)$ be given by Eq. 6 where $h(t, \tau)$ is the solution to (4) subject to the boundary condition $h(t, 0) = g(t)$, $0 \leq t \leq T$, and let $f(s;\mu)$ be the realizable part of the spectrum

$$1 + f(s;\mu) + f(-s;\mu) = \frac{1}{R(s;\mu) R(-s;\mu)}. \quad (9)$$

We can show that the state transition matrix associated with (8) is given by

$$\Phi(\mu, s) = \begin{bmatrix} y_1(\mu, s) & y_2(\mu, -s) \\ y_2(\mu, s) & y_1(\mu, -s) \end{bmatrix}, \quad (10)$$

where

$$y_1(\mu, s) = (1 + f(s;\mu)) R(s;\mu)$$

$$y_2(\mu, s) = -f(-s;\mu) R(-s;\mu).$$

Thus we may solve (8) by obtaining the solution to (4) and factoring the spectrum (9).

We now apply this to the transmission-line problem.

5. Solution of the Nonuniform Transmission Line

Consider a nonuniform lossless transmission line segment on the interval $0 \leq \mu \leq T$ with characteristic impedance $z(\mu)$, where the variable μ represents the two-way propagation time. The Laplace transform $V(\mu, s)$ of the propagating voltage satisfies the differential equation

$$\frac{\partial^2}{\partial \mu^2} V(\mu, s) = 2g(\mu) \frac{\partial}{\partial \mu} V(\mu, s) - \frac{s^2}{4} V(\mu, s), \quad (11)$$

where $g(\mu)$, $0 \leq \mu \leq T$ is the reflection-coefficient density defined by

$$g(\mu) = \frac{1}{2} \frac{\partial}{\partial \mu} \ln(z(\mu)).$$

The corresponding equation for the current follows by replacing $g(\mu)$ with $-g(\mu)$ in (11).

It is easy to verify that

$$V(\mu, s) = \exp\left(\int_0^\mu g(t) dt\right) \left[e^{s\mu/2} \underline{x}_1(\mu, s) + e^{-s\mu/2} \underline{x}_2(\mu, s) \right], \quad (12)$$

where $\underline{x}(\mu, s)$ satisfies the state equation (8). We observe that the first and last terms in brackets in (12) represent voltage waves traveling in backward (-) and forward (+) directions, respectively. Thus defining the voltage vector

$$\underline{V}(\mu, s) = \begin{bmatrix} V_-(\mu, s) \\ V_+(\mu, s) \end{bmatrix}$$

and the delay matrix

JS

JS

(XIV. DETECTION AND ESTIMATION THEORY)

$$\underline{D}(\mu, s) = \begin{bmatrix} e^{s\mu/2} & 0 \\ 0 & e^{-s\mu/2} \end{bmatrix},$$

we may write (12) as

$$\underline{V}(\mu, s) = \exp\left(\int_0^\mu g(t) dt\right) \underline{D}(\mu, s) \underline{x}(\mu, s). \quad (13)$$

Or, employing the state transition matrix (10), we obtain

$$\underline{V}(\mu, s) = \exp\left(\int_0^\mu g(t) dt\right) \underline{D}(\mu, s) \underline{\Phi}(\mu, s) \underline{V}(0, s), \quad (14)$$

which is the desired result. We note that if two additional linear constraints are imposed on the forward and backward components at $\mu = 0$ and $\mu = T$, then (14) completely determines the line voltage.

To provide an example of this and to obtain an analogy to known discrete-time results, we consider the transmission-line segment (Fig. XIV-2) which is terminated in its characteristic impedance and is driven by an impulsive current source.

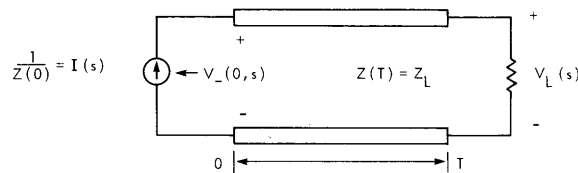


Fig. XIV-2. Transmission-line segment.

We want to compute the load voltage $V_L(s)$ and the backward propagating voltage at the origin $V_-(0, s)$. We observe that the boundary conditions for this problem are

$$V_+(0, s) = 1 + V_-(0, s)$$

$$V_+(T, s) = V_L(s)$$

$$V_-(T, s) = 0.$$

Evaluating (14) at $\mu = T$ and applying the boundary conditions, we obtain

$$V_-(0, s) = f(s; T) \quad (15)$$

$$V_L(s) = \exp\left(\int_0^T g(t) dt\right) e^{-sT/2} \frac{1}{R(s; T)}. \quad (16)$$

The discrete-time version of (15) and (16) is well known in the field of seismology^{11, 12} where the earth strata are regarded as a medium of N reflecting layers for acoustical waves and (15) corresponds to the acoustic response or seismogram of the medium. Our interpretation of $g(t) = h(t, 0)$, $0 \leq t \leq T$ as a reflection-coefficient density is analogous to the interpretation of the partial correlation coefficients as the reflection coefficients of the layers.

6. Chandrasekhar Equations

Consider the Wiener-Hopf integral equation (1) for the special case

$$\beta(\mu, \nu) = \beta(\mu - \nu) = \int_a^b e^{-|\mu - \nu| a} w(a) da.$$

Chandrasekhar³ has shown that the solution $h(t, \tau)$ of this equation can be written in terms of two functions, now known as the Chandrasekhar X and Y functions, satisfying the simultaneous nonlinear differential equations

$$\frac{\partial}{\partial t} X(t, a) = -Y(t, a) g(t) \quad (17)$$

$$\frac{\partial}{\partial t} Y(t, a) = -aY(t, a) - X(t, a) g(t) \quad (18)$$

$$X(0, a) = 1 = Y(0, a), \quad a \leq a \leq b,$$

where

$$g(t) = h(t, 0) = \int_b^a Y(t, a') w(a') da', \quad 0 \leq t \leq T.$$

Since these equations have been given considerable attention,^{2, 3, 13-17} it is of interest to interpret them in terms of the stationarity equation (4).

Comparing (17) and (18) with the state equation (8), we see that

$$X(t, a) = X_1(t, a)$$

$$Y(t, a) = e^{-at} X_2(t, a).$$

Thus the Chandrasekhar equations are related in a simple way to the state equation where s is restricted to be a real variable.

It follows readily from the stationarity equation that

$$\frac{\partial}{\partial t} R(a:t) = -g(t) e^{-at} R(-a:t). \quad (19)$$

(XIV. DETECTION AND ESTIMATION THEORY)

JS

Comparing (19) with (17) and (18) and noting that $R(a:0) = 1$, we see that

$$X(t, a) = R(a:t) \tag{20}$$

$$Y(t, a) = e^{-at} R(-a:t). \tag{21}$$

This is not a solution to (17) and (18) in the usual sense, since we are not given $g(t)$ as in the transmission-line problem. It does, however, provide an interesting interpretation of the X and Y functions and we may conclude that the Chandrasekhar equations are an immediate consequence of the stationarity equation.

7. Summary

We have considered applications of the stationarity equation to spectral estimation and wave propagation in a lossless nonhomogeneous medium and indicated that the Chandrasekhar equations follow readily from this equation.

In the first application we discussed a generalization of the maximum entropy method (M. E. M.) so as to include arbitrary positive-definite extensions of the estimated covariance. This procedure was based on the fact that the continuous positive-definite extensions of $\delta(\tau) + \beta(\tau)$, $|\tau| \leq T$ are equivalent to the continuous extensions of $h(t, 0)$, $0 \leq t \leq T$.

The second application followed from the observation that we could solve a certain distributed-state variable equation. The solution was obtained by solving the stationarity equation and then performing a spectral factorization.

References

1. H. L. Van Trees, Detection, Estimation, and Modulation Theory: Part 1. Detection, Estimation, and Linear Modulation Theory (John Wiley and Sons, Inc., New York, 1968).
2. T. Kailath, "Some New Algorithms for Recursive Estimation in Constant Linear Systems," *IEEE Trans.*, Vol. IT-19, No. 6, pp. 750-759, November 1973.
3. S. Chandrasekhar, "On the Radiative Equilibrium of a Stellar Atmosphere," *Astrophys. J.* 106, 152 (1947); 107, 48 (1948).
4. T. Kailath, "Fredholm Resolvents, Wiener-Hopf Equations, and Riccati Differential Equations," *IEEE Trans.*, Vol. IT-15, No. 6, pp. 665-671, November 1969.
5. E. M. Hofstetter, "An Introduction to the Mathematics of Linear Predictive Filtering as Applied to Speech Analysis and Synthesis," M. I. T. Lincoln Laboratory, Technical Note 1973-36, July 1973.
6. N. Wiener, Extrapolation, Interpolation and Smoothing of Stationary Time Series" (The Technology Press of M. I. T. and John Wiley and Sons, Inc., New York, 1957), Appendix B.
7. J. P. Burg, "Maximum Entropy Spectral Analysis," a paper presented at 37th Annual International SEG Meeting, Oklahoma City, Oklahoma, October 1967.
8. R. T. Lacoss, "Data Adaptive Spectral Analysis Methods," *Geophys.* 36, 661-675 (1971).

JS

(XIV. DETECTION AND ESTIMATION THEORY)

9. E. Parzen, "Multiple Time Series Modeling," Technical Report No. 12 on Contract Nonr-225-(80), Stanford University, Palo Alto, California, July 1968.
10. L. Pusey, "High-Resolution Spectral Estimates" (to be published by M. I. T. Lincoln Laboratory).
11. J. F. Claerbout, "Synthesis of a Layered Medium from Its Acoustic Transmission Response," *Geophys.* 33, 264-269 (1968).
12. G. Kunetz and I. d'Erceville, "Sur Certaines Propriétés d'une Onde Acoustique Plane de Compression dans un Milieu Stratifié," *Ann. Geophys.* 18, 351-359 (1962).
13. J. L. Casti, R. E. Kalaba, and K. Murthy, "A New Initial-value Method for Online Filtering and Estimation," *IEEE Trans.*, Vol. IT-18, No. 4, pp. 515-518, July 1972.
14. J. Casti and E. Tse, "Optimal Linear Filtering and Radiative Transfer: Comparisons and Interconnections," *J. Math. Anal. App.* 40, 45-54 (1972).
15. J. Casti, R. Kalaba, and S. Ueno, "Invariant Imbedding and the Variational Treatment of Fredholm Integral Equations with Displacement Kernels," *J. Math. Phys.* 12, 1276-1278 (1971).
16. J. Buell, J. Casti, R. Kalaba, and S. Ueno, "Exact Solution of a Family of Matrix Integral Equations for Multiple Scattered Partially Polarized Radiation. II," *J. Math. Phys.* 11, 1673-1678 (1970).
17. G. H. Box and G. M. Jenkins, Time Series Analysis Forecasting and Control (Holden-Day, San Francisco, 1970).

B. RANGE ESTIMATION PERFORMANCE WITH NARROW-BAND PASSIVE SIGNALS

Joint Services Electronics Program (Contract DAAB07-71-C-0300)

José M. F. Moura

In this report we analyze adaptive passive systems tracking a moving or a stationary source that radiates a narrow-band signal. We also carry out performance studies based on the Cramer-Rao inequality. The main issue is the range estimation performance, since it has been shown¹ that receivers designed with linearized models (e.g., extended Kalman filters) exhibit fundamental range ambiguity resulting from the narrow-band signal structure and the linearized approximations. We consider two problems of

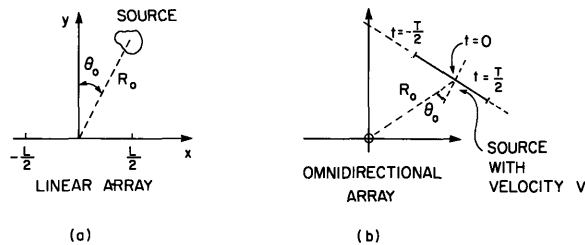


Fig. XIV-3. (a) Stationary array, stationary source (SASS).
(b) Stationary array, moving source (SAMS).

(XIV. DETECTION AND ESTIMATION THEORY)

JS

practical significance and emphasize their space/time dualism. We have (Fig. XIV-3a) the dual problem of a Stationary Array detecting a Stationary Source (SASS), or equivalently a Moving observer generating a synthetic Array tracking a Stationary Source (MASS), and (Fig. XIV-3b) a Stationary omnidirectional Array tracking a Moving Source (SAMS).

1. Signal Model

We assume that the radiations are narrow-band. At any point of the receiving array we model the signal at time t as

$$r(t, \ell) = \sqrt{2} \operatorname{Re} \{ (\tilde{s}(t, \ell) + \tilde{w}(t, \ell)) \exp(-j\omega_c t) \} \tag{1}$$

with the signal complex envelope

$$\tilde{s}(t, \ell) = \left(\frac{E_r}{LT} \right)^{1/2} \tilde{b} \exp \left[j \frac{2\pi}{\lambda} R(t, \ell) \right], \tag{2}$$

where E_r is the total energy received during the observation time interval $\left[-\frac{T}{2}, \frac{T}{2} \right]$ by an array of dimension L ; $R(t, \ell)$ is the distance (range) at time t from the source to the array element at location ℓ ; $\lambda = \frac{2\pi c}{\omega_c}$ is the wavelength; and $\tilde{b} = b \exp[j\psi]$, with b a Rayleigh-distributed random variable, and ψ uniformly distributed in $[0, 2\pi]$. The complex Gaussian random variable \tilde{b} accounts for the absence of an absolute phase reference (incoherent receiver) and makes it explicit in the model that the focusing on the range parameter is to be achieved from the modulation induced in the signal structure rather than from the absolute phase. It also accounts for model inaccuracies caused by variations of the transmitted signal power about some nominal value, fading in the transmission medium, and so forth. The complex additive noise $\tilde{w}(t, \ell)$ is assumed to be spatially and temporarily white Gaussian noise with spectral height N_o .

Case A. Stationary Array – Stationary Source (SASS)

Within the SASS context the range is determined from the spherical curvature of the incoming wave fronts (targets in the near field). We keep the parametrization of Fig. XIV-3a, and for a linear array

$$\frac{2\pi}{\lambda} R(t, \ell) = \frac{2\pi}{\lambda} \left\{ R_o^2 + \ell^2 + 2\ell R_o \sin \theta_o \right\}^{1/2}. \tag{3}$$

Case B. Stationary Array – Moving Source (SAMS) and Moving Array – Stationary Source (MASS)

By assuming planar wave fronts (targets in the far field) and constraining the source

JS

or observer motions to a nominal constant-velocity linear path, the parametrization in Fig. XIV-3b leads to

$$\frac{2\pi}{\lambda} R(t, \ell) = \frac{2\pi}{\lambda} \left\{ R_o^2 + (vt)^2 + 2(vt)R_o \sin \theta_o \right\}^{1/2}. \quad (4)$$

Identification of ℓ with vt in expressions (3) and (4) emphasizes the space/time dualism underlying the range measurement in cases A and B. In the SASS context the spherical curvature of the incoming wave fronts induces a "nonlinear spatial modulation" while in the SAMS or MASS configurations the range information is conveyed by the nonlinear temporal modulation induced on the signal structure by the relative dynamics. Three remarks should be made.

(i) In the general SAMS problem the target speed is unknown and represents an extra parameter to be estimated. The errors are highly correlated with errors in the estimate of the other parameters with the net effect of deterioration in the receiver performance.

(ii) If the parameter v is assumed known, which is realistic in a MASS problem, then the SASS and MASS estimation problems are basically equivalent. But with a moving observer we can synthesize larger arrays by simply enlarging the observation interval. Therefore in practice the ranges of application are much greater than for the spherical curvature measurement processors.

(iii) Expressions (3) and (4) can be approximated by a truncated Taylor's series. It can be shown that within the SASS or MASS contexts (with known velocity) a second-order expansion leads to a range observable model, while in the SAMS problem with an omnidirectional array third-order temporal effects are required to focus on the range parameter. In the sequel we shall work with the general expressions (3) and (4).

2. Performance Bounds

We study the performance bounds derived from the Cramer-Rao inequality. It is well known² that if $\Lambda_\epsilon = \begin{bmatrix} \sigma^2 \\ \sigma_{ij}^2 \end{bmatrix}$ is the error covariance matrix of the parameter estimates, then $\Lambda_\epsilon \geq J^{-1}$, where J is the Fisher Information Matrix (FIM) which for this problem has the general element

$$J_{ij} = \frac{2\tilde{E}_r}{N_o} \frac{\tilde{E}_r}{N_o + \tilde{E}_r} \operatorname{Re} \left\{ \int_{-T/2}^{T/2} dt \int_{-L/2}^{L/2} d\ell \frac{\partial \tilde{s}_n}{\partial A_i} \frac{\partial \tilde{s}_n^*}{\partial A_j} - \left[\int_{-T/2}^{T/2} dt \int_{-L/2}^{L/2} d\ell \frac{\partial \tilde{s}_n}{\partial A_i} \tilde{s}_n^* \right] \left[\int_{-T/2}^{T/2} dt \int_{-L/2}^{L/2} d\ell \frac{\partial \tilde{s}_n}{\partial A_j} \tilde{s}_n^* \right]^* \right\}, \quad (5)$$

where

$$\tilde{s}_n = \frac{1}{\sqrt{LT}} \exp j \frac{2\pi}{\lambda} R(t, \ell, A), \quad t \in \left[-\frac{T}{2}, \frac{T}{2}\right], \quad \ell \in \left[-\frac{L}{2}, \frac{L}{2}\right], \quad A = \begin{bmatrix} R_o \\ v \\ \sin \theta \end{bmatrix},$$

and the star indicates complex conjugate.

By direct substitution and integration we obtain closed-form expressions for FIM and Λ_{ϵ} . Apart from a multiplicative gain G , the elements of FIM depend essentially on the bearing θ and a geometric parameter $X = \frac{vT}{R_o}$ for the SAMS or MASS or $X = \frac{L}{R_o}$ for the SASS problem. Given the analytical complexity of this dependence, we pursue the study by graphical analysis.

We take

$$\begin{aligned} \text{SNR} &= \text{signal-to-noise ratio} = 0 \text{ dB} & v &= 30 \text{ ft/s} \\ G &= \frac{\text{SNR}}{\left(\frac{R_o}{R_o^r}\right)^2} \left(\frac{2\pi}{\lambda}\right)^2 LT & \sigma_{R_o} &= \sqrt{\sigma_{11}^2} = \text{range standard deviation} \\ R_o^r &= 6 \times 10^4 \text{ ft} & \sigma_v &= \sqrt{\sigma_{22}^2} = \text{velocity standard deviation} \\ \lambda &= 50 \text{ ft} & \sigma_{\sin \theta} &= \sqrt{\sigma_{33}^2} = \text{sin } \theta \text{ standard deviation.} \end{aligned}$$

In the expression for the multiplicative gain G it is assumed that $|\tilde{b}|$ is either a known amplitude or an unknown nonrandom amplitude.

For the SAMS and MASS we take $L = 250$ ft and with the SASS configuration we take $T = \frac{250}{30}$ s, so that the gain G will be the same whenever all other parameters and X are equal.

Figure XIV-4 shows the behavior of σ_{R_o} as a function of θ . Comparing Fig. XIV-4a with Fig. XIV-4b, we note a sharp decrease in performance for small bearings in the SAMS problem. This is explained by the strong coupling between the errors in the estimates (skewed error ellipsoids) and the large errors in the velocity estimate, as seen from Fig. XIV-5a. After a certain bearing these errors are sharply reduced with a corresponding gain in σ_{R_o} which then follows the same pattern as in Fig. XIV-4b, monotonically increasing when approaching an end-fire array geometry. This is because of the reduction of the effective synthetic array dimension, which also explains the behavior of $\sigma_{\sin \theta}$ as illustrated in Fig. XIV-5b.

Figure XIV-6 shows the dependence of the range standard deviation on the absolute value of R_o . Under the assumed conditions, and for a proportionately larger observation interval, so that X is constant, the deterioration in performance is essentially due

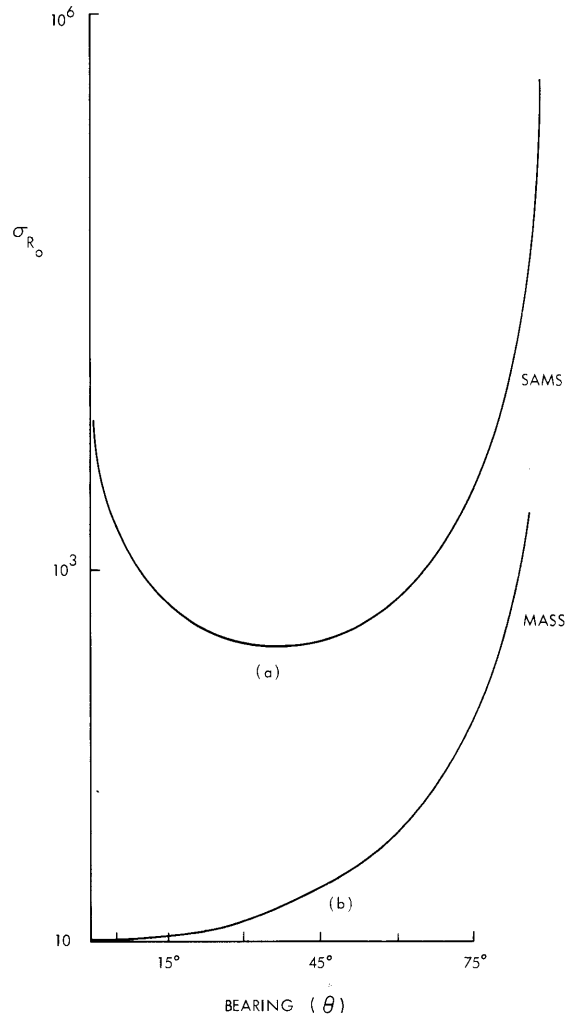


Fig. XIV-4. Range standard deviation as a function of bearing. $R_o = 6 \times 10^4$ ft. $T = R_o/4V$.
 (a) Stationary array - moving source (SAMS).
 (b) Moving array - stationary source (MASS).

JS

JS

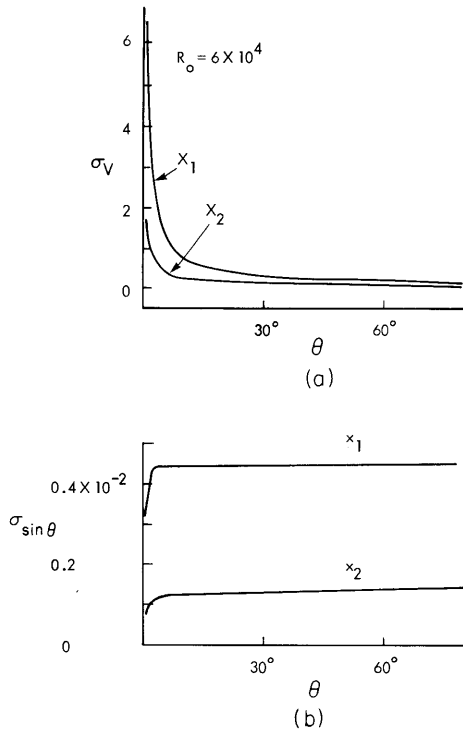


Fig. XIV-5.

- (a) Velocity standard deviation as a function of bearing (SAMS).
- (b) Bearing standard deviation as a function of bearing (SAMS). $X_1 = 1/5.4$, $X_2 = 0.25$.

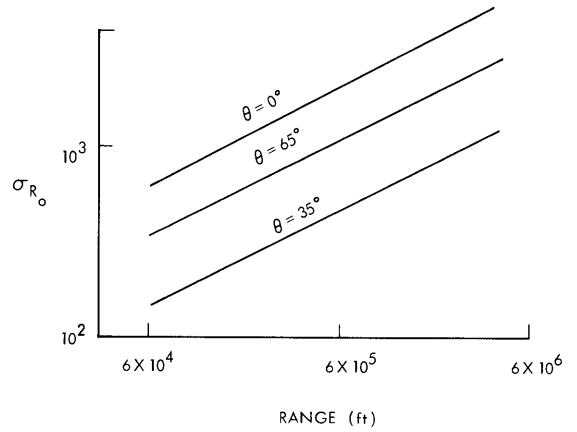


Fig. XIV-6.

Range standard deviation as a function of range (SAMS). $R_0 = 6 \times 10^4$ ft. $\frac{vT}{R_0} = \frac{1}{5.74}$.

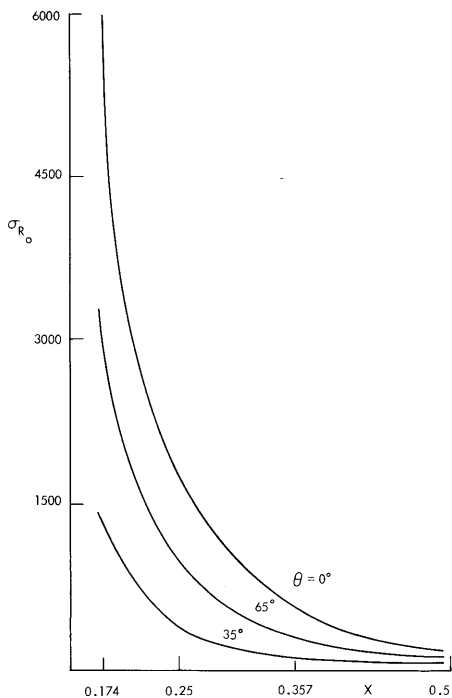


Fig. XIV-7.

Range standard deviation as a function of $X = vT/R_0$ (SAMS). $R_0 = 6 \times 10^4$ ft.

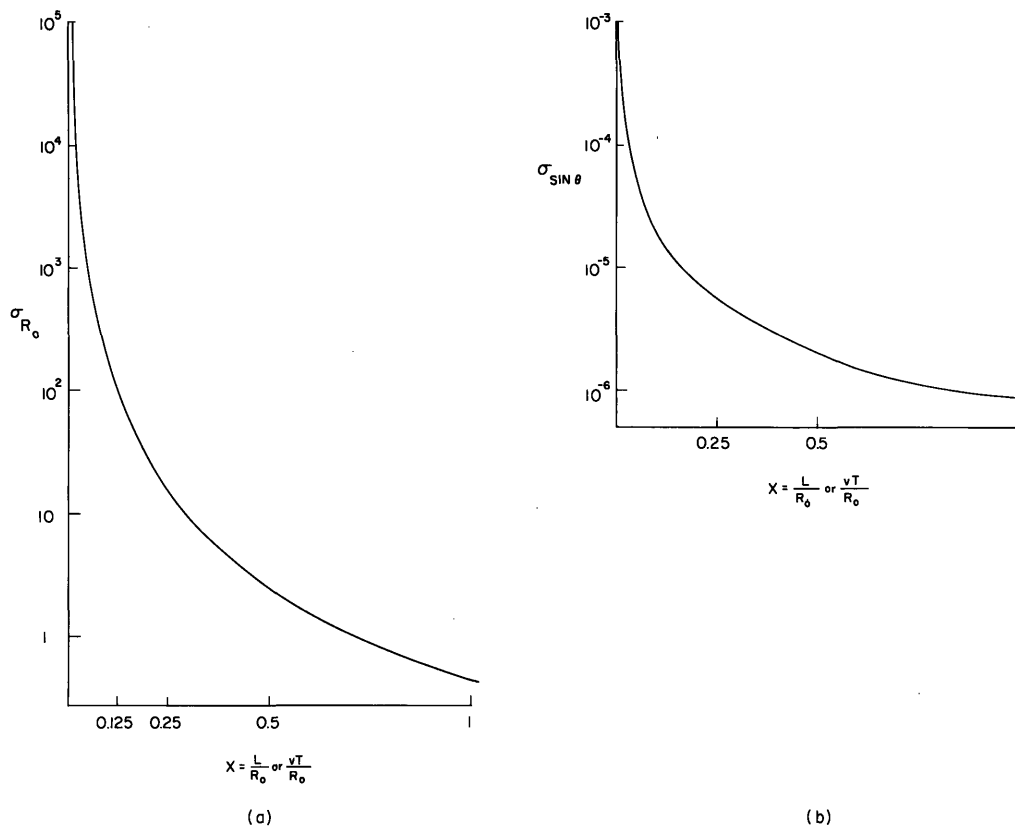


Fig. XIV-8. (a) Range and (b) bearing standard deviation as functions of X (SASS or MASS). $R_o = 6 \times 10^4$ ft, $\theta = 35^\circ$.

to the signal power dependence on the normalized inverse of the range squared.

Figure XIV-7 illustrates the behavior of the range standard deviation with the parameter X, namely, a strong deterioration for small X while saturating for X near 0.5. Figure XIV-8 shows the equivalent behavior of σ_{R_o} and $\sigma_{\sin \theta}$ for the SASS and MASS problems. We note, however, the gain in performance when going from a SASS to a MASS configuration. But for ranges of the order of 10 miles or greater the X parameter will be very small for the SASS problem; that is, we are usually at the left ends of Fig. XIV-8a and 8b.

References

1. J. M. F. Moura, H. L. Van Trees, and A. B. Baggeroer, "Space/Time Tracking by a Passive Observer," Proc. Fourth Symposium on Nonlinear Estimation Theory and Its Applications, September 10-12, 1973, San Diego, California.
2. H. L. Van Trees, Detection, Estimation, and Modulation Theory: Part 1. Detection, Estimation, and Linear Modulation Theory (John Wiley and Sons, Inc., New York, 1968).

